Front. Optoelectron. 2013, 6(3): 290–296
DOI 10.1007/s12200-013-0335-9

RESEARCH ARTICLE

Design optimization of microwave properties for polymer electro-optic modulator using full vectorial finite element method

Kambiz ABEDI (✉), Habib VAHIDI

Department of Electrical Engineering, Faculty of Electrical and Computer Engineering, Shahid Beheshti University, Tehran 1983963113, Iran

Abstract In this paper, a polymer electro-optic modulator has been designed and optimized using the full vectorial finite element method. For this purpose, the effects of magnesium oxide (MgO) and down cladding thicknesses, distance between two ground electrodes, hot electrode and modulator widths modulator on the key modulator parameters, such as microwave effective index n_m, the characteristic impedance Z_C and the microwave losses α are presented. After selecting optimal dimensions of polymer electro-optic modulator, frequency dependent aforementioned parameters and the half-wave voltage-length product ($V_\pi L$) parameter of polymer electro-optic modulator are extracted and as a consequence, an optimized design is reported. Finally, the optical and electrical modulation responses of polymer electro-optic modulator are calculated. The optimized polymer electro-optic modulator exhibits 3-dB electrical bandwidth of 260 GHz and $V_\pi L$ about 2.8 V·cm in this frequency.

Keywords electro-optic modulators, finite element method, integrated optics, optical communication

1 Introduction

Optical modulators play an important role in all optical communication systems. These devices can be categorized into two main groups of electroabsorption and electro-optic modulators. Electro-optic modulators have a variety of advantages over electroabsorption modulators, and therefore they are under investigation more than electro-absorption modulators. To realize high bandwidth in electro-optic modulators, we should match the velocities of microwave and optical wave with each other. The line characteristic impedance should be also matched with the source and load impedances that are usually 50 Ω. Meanwhile, the microwave loss of dielectrics and conductors should be decreased. In addition to bandwidth, the drive voltage is another important parameter in electro-optic modulators, which must be as low as possible. This voltage is dependent on the electro-optic coefficient of used electro-optic material and to the interaction of microwave and optical wave [1–9]. If we increase the interaction, the dielectric and conductor losses will be dominant, and in spite of speeds and impedances matching, we will have small bandwidth. Therefore, we must choose another way to increase the bandwidth and the only remaining way is to increase the electro-optic coefficient. The electro-optic material has the electro-optic coefficient around 30 pm/V, which is suitable to build low voltage wide bandwidth modulators. If we are interested in larger bandwidths with the low drive voltages, we have to use materials with larger electro-optic coefficients. The commonly used materials for this reason are electro-optic polymers. The early polymer materials were suffered from low thermal and photo stability such that the high electro-optic coefficient of them reduced over the time. But new materials such as CLD-1/APC polymers show good stability of the electooptic coefficient and very large electro-optic coefficient (92 pm/V) and therefore are appropriate for our purpose [1]. Some works with this material attain to bandwidths about 170 GHz for drive voltage of 3 V·cm [3]. But since this material with this large electro-optic coefficient has potentials over these results, we have optimized one of structures that proposed in Ref. [1] with some basic variation and utilizing CLD-1/APC as electro-optic material to achieve larger bandwidth and lower voltage.

Received April 22, 2013; accepted June 20, 2013

E-mail: K_Abedi@sbu.ac.ir

2 Modulator layout and cross-section

The cross-section of polymer electro-optic modulator that we have designed and optimized in this work is shown in Fig. 1. The core material is the CLD-1/APC polymer. Ribs are formed on top of the core material with dimensions such that the single mode operation is preserved [3]. Two claddings of UFC-170 and UV-15 materials are placed on top and at bottom of this material as upper and lower cladding, respectively. These claddings, in addition to prepare good optical confinement with having lower refractive indexes than CLD-1/APC, didnot physically degrade solvent sensitive CLD-1/APC at their common boundaries [1]. Below the down cladding, a layer of magnesium oxide, MgO, has been placed. This material has large relative permittivity (about 9.8) that helps us in good speed matching between microwave and optical wave [2].

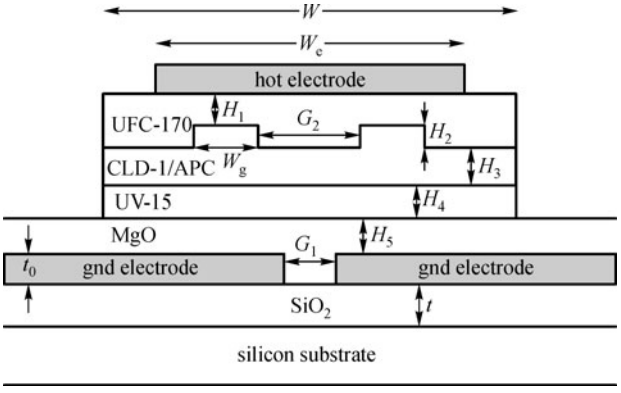

Fig. 1 Schematic cross-section of polymer electro-optic modulator

Two splitted ground electrodes placed below this MgO material that altogether placed on top of the silicon substrate via one SiO_2 layer. One hot electrode also placed on the top of these layers. The refractive index and relative permittivity of all utilized materials have been listed in Table 1.

Some differences of our structure with Ref. [3] are extending ground electrode and it is above layer from sides, using MgO material to achieve good matching, taking different width of hot electrode with respect to modulator width and decreasing distance between hot and ground electrodes to lowering $V_\pi L$. Furthermore, we have used more dimension in optimization and achieved to better matching and lower attenuation.

Table 1 Relative permittivity and refractive indexes of utilized materials

material	refractive index	permittivity
UFC-170	1.488	2.5
CLD-1/APC	1.612	3.0
UV-15	1.504	2.5
SiO_2	1.460	3.9
MgO	1.730	9.8
silicon	3.880	11.7

3 Numerical technique

In determining frequency response of one modulator, it is necessary to calculate some parameters. These parameters include microwave effective index, n_m, characteristic impedance, Z_C, microwave attenuations, α, and optical effective index, n_{eff}. From these parameters, the response of the modulator can be calculated using Eq. (1) in which l is the length of the modulator that for our modulator is 1 cm, c is the velocity of the light in vacuum, Z_1 and Z_2 are source and load impedances and f is the frequency [3,10]. The dB electrical response can be determined by $20\log m(f)$ whilst the dB optical response can be determined by $10\log m(f)$.

$$m(f) = \left| \frac{1 - S_1 S_2}{(1 + S_2)[e^{2ju_+} - S_1 S_2 e^{-2ju_-}]} \times \left[e^{ju_+} \frac{\sin u_+}{u_+} + S_2 e^{-ju_-} \frac{\sin u_-}{u_-} \right] \right|, \quad (1)$$

where

$$S_1 = \frac{Z_1 - Z_C}{Z_1 + Z_C}, S_2 = \frac{Z_2 - Z_C}{Z_2 + Z_C}, \quad (2a)$$

and

$$u_\pm = \frac{1}{c} f l (n_m \mp n_{eff}) - j\frac{1}{2}\alpha. \quad (2b)$$

The only remaining parameter is the drive voltage of the modulator, $V_\pi L$, which can be defined as the voltage needed to produce 180° phase difference in two arms of Mach-Zehnder (MZ) modulator [7]. This voltage can be evaluated using relation

$$V_\pi L = \frac{\pi V_0}{\Delta\beta}, \Delta\beta = \beta_1 - \beta_0, \quad (3)$$

where, V_0 is the applied voltage, and β_1 and β_0 are the propagation constants of the light with and without the modulating electric field. From all required parameters in determining response and voltage of the modulator, n_m, α, Z_C and the modulating electric field must be obtained by microwave analysis, and n_{eff}, β_0 and β_1 by optical analysis. Also one quasi- transverse electromagnetic (TEM) is required to calculate modulating electric field that causes Δn and so $\Delta\beta$.

We used the full vectorial finite element method in microwave analysis and quasi-transverse magnetic finite element method (TM FEM) analysis in order to do optical

analysis.

The vectorial FEM is based on the edge element formulation [10–14]. The most important advantage of using edge element finite element formulation is to prevent from the appearance of spurious modes [12]. This avoidance will be achieved along with some problems such as loosing sparsity of matrices [14] that prevent us from taking advantage of sparse matrix solver algorithms [15] in solving eigenvalue equation. If we are going to use these algorithms in edge-element formulations, we must use full wave in such a way that the size of our matrices increase from $e \times e$, in which e is total number of edges, to $(e+n) \times (e+n)$, in which n is total number of nodes, as done in Refs, [10,11]. Although spurious modes can be removed by some technique in nodal FEM, such as introducing penalty parameter [13], however this cause some error and dependency of our results to proper choice of penalty parameter [13].

The edge element formulation can be extracted from discretization of vector wave equation of

$$\nabla \times \nabla \times E - k_0^2[\varepsilon_r]E = 0. \tag{4}$$

By discretization and applying FEM procedure, the following eigenvalue equation extracted

$$[K_{tt}]\{E_t\} - \gamma^2([M_{tt}] + [K_{tz}][K_{zz}]^{-1}[K_{zt}])\{E_t\} = \{0\}, \tag{5}$$

with

$$\begin{aligned}[K_{tt}] = \sum_e \iint_e [&\varepsilon_x k_0^2 \{U\}\{U\}^T + \varepsilon_y k_0^2 \{V\}\{V\}^T \\ &- \{U_y\}\{U_y\}^T - \{V_x\}\{V_x\}^T \\ &+ \{U_y\}\{V_x\}^T + \{V_x\}\{U_y\}^T]\mathrm{d}x\mathrm{d}y,\end{aligned} \tag{6a}$$

$$\begin{aligned}[K_{tz}] &= [K_{zt}]^T \\ &= \sum_e \iint_e [\{U\}\{N_x\}^T + \{V\}\{N_y\}^T]\mathrm{d}x\mathrm{d}y,\end{aligned} \tag{6b}$$

$$\begin{aligned}&[K_{zz}] \\ &= \sum_e \iint_e [\varepsilon_z k_0^2 \{N\}\{N\}^T - \{N_x\}\{N_x\}^T - \{N_y\}\{N_y\}^T]\mathrm{d}x\mathrm{d}y,\end{aligned} \tag{6c}$$

$$[M_{tt}] = \sum_e \iint_e [\{U\}\{U\}^T + \{V\}\{V\}^T]\mathrm{d}x\mathrm{d}y. \tag{6d}$$

$\{E_t\}$ is the transverse value of electric field at all edges and $\gamma = \beta - \mathrm{j}\alpha$ is complex propagation constant. The shape functions $\{N\}$, $\{U\}$ and $\{V\}$ are illustrated in Ref. [12].

The longitudinal component can be computed from transverse components by

$$\{E_z\} = \gamma[K_{zz}]^{-1}[K_{zt}]\{E_t\}. \tag{7}$$

By obtaining the eigenvalue, the microwave effective index can be obtained from

$$n_m = \mathrm{Re}(\gamma)/k_0 = \beta/k_0. \tag{8}$$

And the attenuation constant in Neper per meter from

$$\alpha = \alpha_c + \alpha_d = \mathrm{Im}(\gamma), \tag{9}$$

where α_c and α_d are the conductor and dielectric loss parameters, respectively. The characteristic impedance of the transmission line in this case should be evaluated using the power current definition in the form of [10]

$$Z_C = \frac{2P}{|I|^2}, \tag{10}$$

where P is modal power and I is the total current in z direction carried by center electrode. P and I in the FEM formulations can be evaluated by [10]

$$\begin{aligned}P &= \frac{1}{2}\iint (E \times H^*) i_z \mathrm{d}x\mathrm{d}y \\ &= \frac{\beta^*}{\omega\mu_0}(\{E_t\}^T[M_{tt}]\{E_t\}^* + \{E_t\}^T[M_{tz}]\{E_z\}^*),\end{aligned} \tag{11a}$$

$$I = \iint \sigma E_z \mathrm{d}x\mathrm{d}y = \sum_e \iint_e \mathrm{j}\beta\sigma\{N\}^T\{E_z\}_e \mathrm{d}x\mathrm{d}y, \tag{11b}$$

where for P, the integration carried out over entire waveguide cross section, whereas for I is done only on hot electrode cross section with conductivity of σ.

After this microwave analysis, the optical analysis is necessary to obtain n_{eff} and $V_\pi L$. To utilize the large electro-optic coefficient (92 pm/V) of CLD-1/APC which is r_{33}, transverse magnetic (TM) polarization is assumed throughout this paper [3].

The optical analysis also could be from full-vectorial type. However, in most of cases, the quasi-TE and quasi-TM analysis work properly. In this paper that TM polarization assumed, the quasi-TM formulation can be used that is based on the following abstraction of wave equation [10].

$$\frac{1}{n_y^2}\frac{\partial^2 H_x}{\partial x^2} + \frac{1}{n_z^2}\frac{\partial^2 H_x}{\partial y^2} - \frac{\beta^2}{n_y^2}H_x + k_0^2 H_x = 0. \tag{12}$$

By applying the FEM to Eq. (12), the following eigenvalue equation can be obtained

$$[K]\{H_x\} = \beta^2[M]\{H_x\}. \tag{13}$$

In which, the vector $\{H_x\}$ is the magnetic field in all element nodes and β is the propagation constant and matrixes $[K]$ and $[M]$ are given with below relations [10].

$$[K] = \sum_e \iint_e \left(k_0^2 \{N\}\{N\}^T - \frac{1}{n_y^2}\frac{\partial\{N\}}{\partial x}\frac{\partial\{N\}^T}{\partial x} \right.$$

$$-\frac{1}{n_z^2}\frac{\partial\{N\}}{\partial y}\frac{\partial\{N\}^{\mathrm{T}}}{\partial y}\Bigg)\mathrm{d}x\mathrm{d}y, \tag{14a}$$

$$[M]=\sum_e\iint_e\frac{1}{n_y^2}\{N\}\{N\}^{\mathrm{T}}\mathrm{d}x\mathrm{d}y. \tag{14b}$$

From calculated eigenvalue β, optical effective index will be $n_{\mathrm{eff}}=\beta/k_0$, where k_0 is wavenumber of the optical wave. This β is the propagation constant of the light without the modulating electric field. Furthermore, since n_y and n_z components influence from electro-optic property of core material through microwave modulating electric field component of E_y. Then, the β_1 can be evaluated from another quasi-TM analysis with the modulating electric field. Consequently,$V_\pi L$ can be determined from Eq. (3).

4 Results and discussion

In this section, we use the full vectorial finite element method to calculate the microwave parameters. For this purpose, the dimensions that affect the optical parameter of n_{eff} are kept unchanged and constant n_{eff} is calculated. Then other parameters are designed to match n_{m} with the constant n_{eff} and characteristic impedance with 50 Ω. We are free in this design except that we should not reduce interaction strength by extra increasing of layers thickness that cause additional $V_\pi L$ enlargement. The parameters that affect n_{m} are type of core and claddings material that not changed at all. Dimensional affecting parameters are H_1, H_2, H_3, H_4, W_{g} and G_2. The width of modulator, W, has negligible effect on n_{eff} and changed during optimization. Among other parameters, only H_4 changed. H_4 is the thickness of down cladding and will influence n_{eff} when its thickness is very small. Therefore, this thickness always is larger than 1.5 μm and thus changing of H_4 didnot affect n_{eff} severely to be needed updating optical analysis. Inadequate parameters restrict our freedom in playing with n_{m}, Z_{C} and α values. We must change such amount of dimensions that lead to independent alteration of each of these three values. We chose five parameters of G_1, H_4, H_5, W and W_{e}.

Figures 2(a)–2(e) show the results of varying these parameters on three major microwave characteristics. It can be observed that as G_1 is increased, the effective index and characteristic impedance values are increased, whereas microwave attenuation values are approximately constant (see Fig. 2(a)). It is also shown that as H_4 is reduced; the effective index and microwave attenuation values are increased, whereas the characteristic impedance values are reduced (Fig. 2(b)). Figure 2(c) also shows the variations of the n_{m} and Z_{C} and α with H_5. It can be noted that n_{m} and Z_{C} decreased as H_5 was decreased. It can also be noted that α increased as H_5 was decreased. With increasing of the W and W_{e} values, n_{m} values are increased, but Z_{C} values are decreasd and microwave attenuation values are approximately constant (Figs. 2(d) and 2(e)). The purpose of these figures is not to precisely study dimensional effects and they only intended to show the behavior of characteristics with respect to these dimensions change. After perceiving these behaviors, we can easily start with one initial dimension values and go ahead through these figures to obtain desirable decrease/increase in n_{m}, Z_{C} and α together with or separately.

Note that all other parameters in these figure is the same dimensions that listed in Table 2. Table 2 shows these final optimized dimension values. All these figures were obtained by the full vectorial FEM in the frequency of 250 GHz. The final dimensions are such that two ribs were exactly between top and ground electrodes in expose of maximum static electric field and therefore $V_\pi L$ be the minimum. After final selecting of dimensions, through one microwave quasi-TEM and two optical quasi-TE analyses, the dc value of $V_\pi L$ can be calculated [5].

For these parameters, the value of n_{eff} computed from quasi-TM analysis is about 1.59. As seen in Fig. 3, the n_{m} is completely matched with n_{eff} value for large frequencies. We have done our full vectorial analysis in 26 points from 10 to 260 GHz with steps of 10 GHz. Utilizing MgO brings this good n_{m} increasing to establish matching with n_{eff}.

The other parameter calculated from microwave analysis is Z_{C}, which is shown in Fig. 4. As we can see from this figure, Z_{C} is nearly matched with 50 Ω in large frequencies. About 0.5 Ω difference of it with 50 Ω has very negligible effect on modulator bandwidth; for this reason, we didnot make more efforts on its full matching.

The microwave attenuation vs frequency that resulted for optimized modulator is displayed in Fig. 5. One rule of thumb that is common for estimating electrical bandwidth of modulators is that when velocities and impedances were matched, the cut-off frequency is wherever the microwave attenuation reaches to the value of 6.5 dB/cm. Then before we begin choosing and optimizing layers materials and

Table 2 Various dimensions of optimized modulator

modulator structure parameter	value/μm
W	38
W_{e}	20
W_{g}	3.5
t	2
t_{e}	2
G_1	6
G_2	8
H_1	1.5
H_2	1
H_3	2
H_4	1.7
H_5	2.6

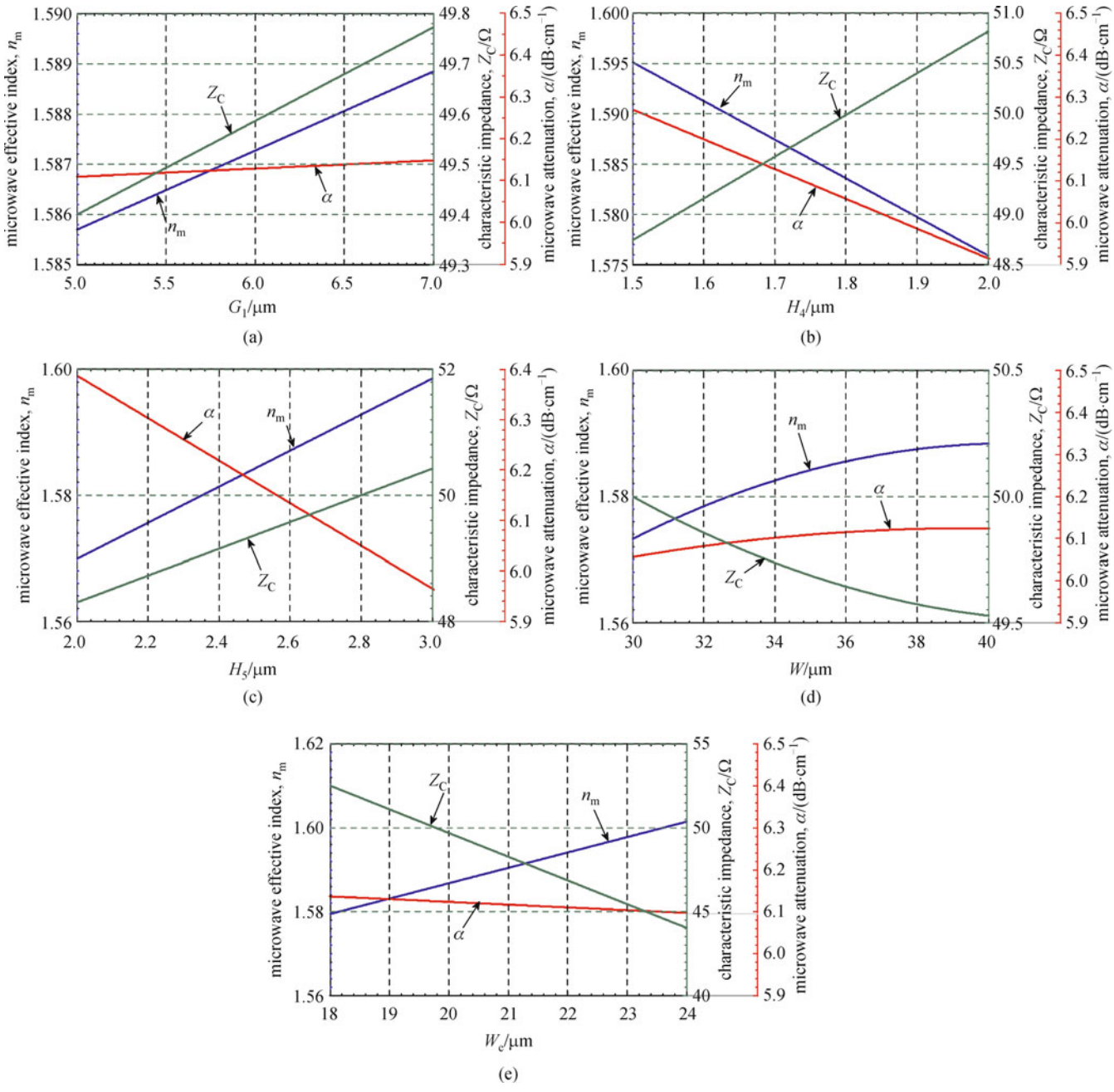

Fig. 2 Results of varying (a) G_1; (b) H_4; (c) H_5; (d) W and (e) W_e on microwave important parameters of n_m, Z_C and α

dimensions, we should take a look that is it possible to have below 6.5 dB/cm losses for one desired $V_\pi L$ or not.

The final modulator response is shown in Fig. 6. It is evident from this figure that the electrical bandwidth of modulator is 260 GHz. From Ref. [3], the dc value of $V_\pi L$ was computed about 2 V·cm. The frequency dependent $V_\pi L$ can be obtained from Ref. [3].

$$V_\pi L(f) = V_\pi L(\mathrm{dc}) 10^{-m(f)/10}. \quad (15)$$

In which, $m(f)$ is dB optical response of the modulator. As we can see from Fig. 7, $V_\pi L$ for 260 GHz frequency is about 2.8 V·cm that is lower than similar works [3].

5 Conclusions

In this paper, we designed and optimized an ultra wideband and low drive voltage polymer electro-optic modulator. For this purpose, frequency dependencies of all important parameters, such as microwave effective index, microwave

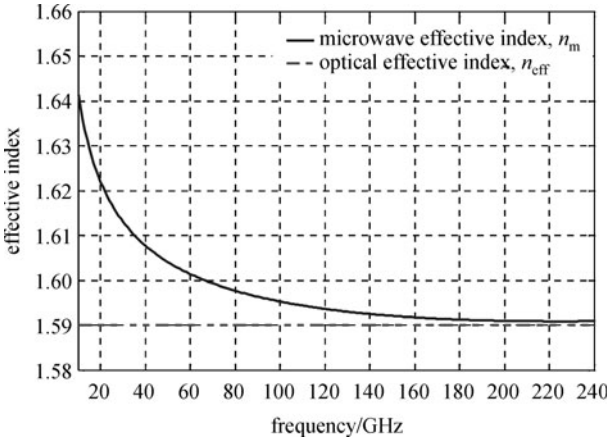

Fig. 3 Microwave effective index vs frequency along with constant optical effective index

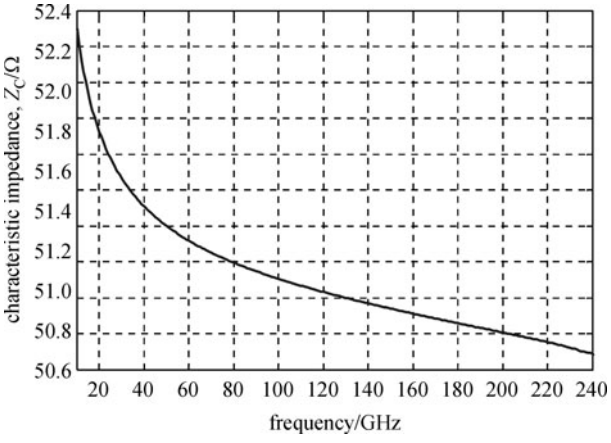

Fig. 4 Characteristic impedance of modulator vs frequency

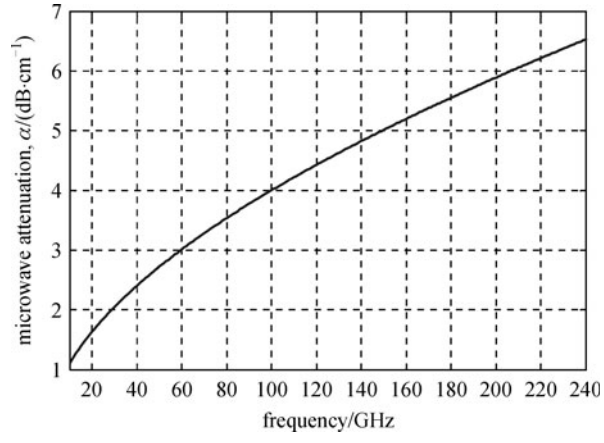

Fig. 5 Microwave attenuation vs frequency

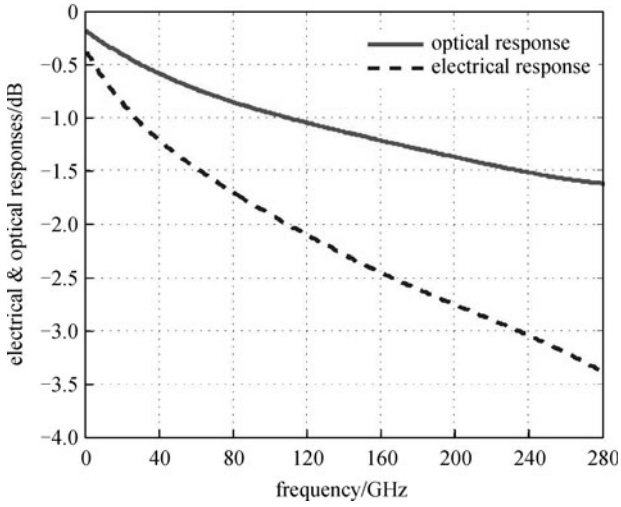

Fig. 6 Electrical and optical responses of modulator vs frequency

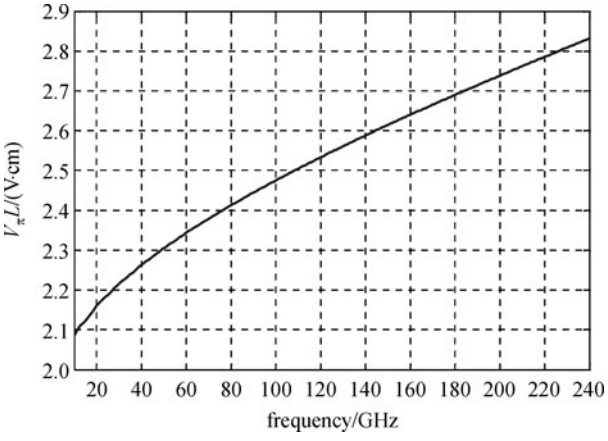

Fig. 7 Frequency dependent the half-wave voltage-length product $V_\pi L$ parameter of modulator vs frequency

characteristic impedance and microwave loss, were extracted. Calculated modulator responses showed an electrical bandwidth of 260 GHz and drive voltage of about 2.8 V · cm in this frequency that is lower than similar works that achieved to lower bandwidths.

References

1. Zhang C, Dalton L R, Oh M C. Low V_π electrooptic modulators from CLD-1 chromophere design and synthesis, material processing, and characterization. Chemistry of Materials, 2001, 13(9): 3043–3050
2. Abedi K, Vahidi H. A polymer electro-optic modulator with ultra wide-band and low driving voltage. Optoelectronics Letters, 2011, 7 (6): 423–426

3. Gorman T, Haxha S, Ju J J. Ultra-high-speed deeply etched electrooptic polymer modulator with profiled cross section. IEEE Journal of Lightwave Technology, 2009, 27(1): 68–76
4. Cui Y, Berini P. Modeling and design of GaAs traveling-wave electrooptic modulators based on the planar microstrip structure. IEEE Journal of Lightwave Technology, 2006, 24(6): 2368–2379
5. Obayya S S A, Haxha S, Rahman B M A, Themistos C, Grattan K T V. Optimization of the optical properties of a deeply etched semiconductor electrooptic modulator. IEEE Journal of Lightwave Technology, 2003, 21(8): 1813–1819
6. Rahman B M A, Haxha S. Optimization of microwave properties for ultrahigh-speed etched and unetched lithium niobate electrooptic modulators. IEEE Journal of Lightwave Technology, 2002, 20(10): 1856–1863
7. Gorman T, Haxha S. Thin layer design of X-cut lithium niobate electrooptic modulator with slotted SiO_2 substrate. IEEE Photonics Technology Letters, 2008, 20(2): 111–113
8. Gorman T, Haxha S. Design optimization of Z-cut lithium niobate electrooptic modulator with profiled metal electrodes and waveguides. IEEE Journal of Lightwave Technology, 2007, 25(12): 3722–3729
9. Gill D M, Chowdhury A. Electro-optic polymer-based modulator design and performance for 40 Gb/s system applications. IEEE Journal of Lightwave Technology, 2002, 20(12): 2145–2153
10. Abedi K, Vahidi H. Structure and microwave properties analysis of substrate removed GaAs/AlGaAs electro-optic modulator structure by finite element method. Frontiers of Optoelectronics, 2013, 6(1): 108–113
11. Saitoh K, Koshiba M. Full-Vectorial finite element beam propagation method with perfectly matched layers for anisotropic optical waveguides. IEEE Journal of Lightwave Technology, 2001, 19(3): 405–413
12. Koshiba M, Maruyama S, Hirayama E. A vector finite element method with the high-order mixed-interpolation-type triangular elements for optical waveguide problems. IEEE Journal of Lightwave Technology, 1994, 12(3): 495–502
13. Lucić R, Bernadić A, Jurić-Grgić I. FEM analysis for MTL problems in frequency domain. International Review on Modelling and Simulations (IREMOS), 2009, 2(3): 249–253
14. Koshiba M, Inoue K. Simple and efficient finite element analysis of microwave and optical waveguides. IEEE Transactions on Microwave Theory and Techniques, 1992, 40(2): 371–377
15. Arroyo J, Zapate J. Subspace iteration search method for generalized eigenvalue problems with sparse complex unsymmetrc matrices in finite-element analysis of waveguides. IEEE Transactions on Microwave Theory and Techniques, 1998, 46(8): 1115–1123